Dielectric and piezoelectric properties of (0.97-x) $Bi_{1/2}Na_{1/2}TiO_3$-$xBi_{1/2}K_{1/2}TiO_3$-0.03$NaNbO_3$ ceramics

YING YUAN, SHUREN ZHANG, JINGSONG LIU
School of Microelectronic and Solid-state Electronics, University of Electronic Science and Technology of China, Jianshe Road, Chengdu, 610054, People's Republic of China

Published online: 12 April 2006

Ceramics of the series (0.97-x)$Bi_{1/2}Na_{1/2}TiO_3$-$xBi_{1/2}K_{1/2}TiO_3$-0.03$NaNbO_3$ ($x = 0$, 0.02, 0.06, 0.10, 0.16, 0.20, 0.30) were prepared by the conventional mixed oxide method. Influence of $Bi_{1/2}K_{1/2}TiO_3$ content on the crystal structure, microstructure, dielectric and piezoelectric properties were studied. All compositions showed single perovskite phase and the morphotropic phase boundary (MPB) between rhombohedral and tetragonal phase existed at the point of $x = 0.16$. Temperature dependences of permittivity and dissipation factor of unpoled samples revealed that permittivity increased with $Bi_{1/2}K_{1/2}TiO_3$ content and it reached maximum value near the MPB. At the same time, the peak value of dissipation factor increased with the addition of $Bi_{1/2}K_{1/2}TiO_3$. All the samples experienced two phase transitions: from ferroelectric to antiferroelectric at the first transition temperature (T_d) and from antiferroelectric to paraelectric at the temperature (T_m) corresponding to maximum value of permittivity. The phase transition from ferroelectric to antiferroelectric had relaxor characteristic and T_d shifted to lower temperature while increasing $Bi_{1/2}K_{1/2}TiO_3$ content. The best piezoelectric properties were obtained in 0.81$Bi_{1/2}Na_{1/2}TiO_3$-0.16$Bi_{1/2}K_{1/2}TiO_3$-0.03$NaNbO_3$ ceramic with a piezoelectric constant (d_{33}) of 146pC/N, planar electromechanical coupling factor (k_p) of 30.3% and thickness electromechanical coupling factor (k_t) of 53.2%. Abnormal piezoelectric properties were observed in the sample ($x = 0.20$), which was attributed to the co-existence of ferroelectric and antiferroelectric phases in it.

1. Introduction

Currently, the most widely used piezoelectric materials are $PbTiO_3$-$PbZrO_3$ three component ceramics (PZT system). However, lead-free piezoelectric ceramics have attracted considerable attention because of their outstanding advantages in free control atmosphere and no lead pollution. $Bi_{1/2}Na_{1/2}TiO_3$ (BNT), discovered by Smolensky [1], is considered to be a promising candidate as lead-free piezoelectric ceramic because it exhibits strong ferroelectricity at room temperature with a large remanent polarization (P_r) of 38 μC/cm [2]. Complex phase transition behaviors are observed in BNT ceramic, which have been debated drastically by many researchers. It is proved that BNT is ferroelectric with rhombohedral symmetry at room temperature. Some researchers concluded that the low temperature phase transition around 220°C marks the transition from the ferroelectric to the antiferroelectric phase. Transition from the antiferroelectric to the paraelectric phase (tetragonal) occurs at 320°C and to cubic phase at 520°C [2, 3]. However, other researchers considered that a strong diffuse phase transition takes place in a wide temperature range from 220°C to 320°C, in which both rhombohedral and tetragonal phase coexist, accompanied with the growth of polar micro regions [4, 5]. BNT has been modified with many dopants, such as $BaTiO_3$ [6], $NaNbO_3$ [7], $BiFeO_3$ [8], Bi_2O_3 Sc_2O_3 [9, 10], La_2O_3 [11], and CeO_2 [12]. It is difficult to pole BNT without doping because of its large coercive field (E_c = 73 kV/cm) and high conductivity at high temperatures.

$Bi_{1/2}K_{1/2}TiO_3$ (BKT) is another well-known lead-free piezoelectric material with a tetragonal symmetry. The solid solution of $(1-x)$ $Bi_{1/2}Na_{1/2}TiO_3$-x$Bi_{1/2}K_{1/2}TiO_3$ has been studied by Sasaki *et al.* [13]. There is the rhomobohedral-tetragonal MPB in the case of $x = 0.16$–0.20. Maximum values of electromechanical coupling factor and the permittivity were observed at MPB, such as k_P = 31.4% and $k_t = 42.3\%$ at $x = 0.16$, and $\varepsilon_{33}^T/\varepsilon_0 = 1030$ at $x = 0.20$.

$BaTiO_3$ (BT), as the third component, has been introduced to BNT-BKT solid solution system and resulted in

0022-2461
DOI: 10.1007/s10853-005-5620-6

large piezoelectric constant (d_{33} = 191 PC/N) and high Curie temperature (T_c = 301°C) at MPB [14]. It is well known that the widely uesd PZT ceramic is the solid solution of ferroelectric $PbTiO_3$ andantiferroelectric $PbZrO_3$. Similarly, antiferroelectric $NaNbO_3$ was introduced to BNT-BKT system with fixed $NaNbO_3$ (NN) content of 0.03, because a maximum remanent polarization (P_r) of 32.6 μC/cm^2 and piezoelectric constant (d_{33}) of 71.1 pC/N were obtained at $x = 0.03$ in $(1-x)$ BNT-xNN system [7]. Thus, a new kind of lead free piezoelectric ceramic with compositions of (0.97-x) BNT-xBKT-0.03NN (x = 0.02, 0.06, 0.10, 0.16, 0.20, 0.30, abbreviated to BNKN100x) were obtained in this study. Moreover, the influence of BKT content on the crystal structure, microstructure, dielectric and piezoelectric properties were investigated.

2. Experimental procedure

A conventional ceramic fabrication technique was used to prepare BNKN system ceramics. Reagent grade oxide or carbonate powders of Bi_2O_3, TiO_2, Nb_2O_5, Na_2CO_3 and K_2CO_3 were used as starting materials. Raw materials were mixed in ethanol with stabilized zirconia balls by ball milling for 24 h. After drying, the mixed powders were calcined at 800–850°C for 2–4 h. The calcined powders were ground again by ball milling for 6 h and pressed into disks of 10 mm diameter and 1mm thickness. Then disks were sintered at 1150°C –1200°C for 2 h in air. X-ray diffraction (XRD) analyses were carried out to check the crystal structure using a Rigaku diffractmeter. Microstructures of the sintered samples were observed using a Hitachi S-530 scanning electron microscope (SEM).

Silver paste was fired on both faces of the discs at 650°C as electrodes. The specimen for measurement of piezoelectric properties was poled in silicon oil at 60°C under a DC field of 50 to 70 kV/cm for 10 min. After poling, a piezo-d_{33} meter (ZJ-3) was used to measure the piezoelectric constant (d_{33}) at 50 Hz. The resonance measurements were performed using an impedance analyzer (Agilent 4294A). The electromechanical coupling factors, such as k_p and k_t, were calculated from the resonance and the anti-resonance frequencies according to Onoe's formula [15]. Temperature dependences of permittivity and dissipation factor of the unpoled samples were measured using a programmable furnace with a LCR meter (HP 4192A), in order to determine the first transition temperature (T_d) and the temperature (T_m) corresponding to the maximum value of permittivity. The free permittivity and dissipation factor of poled samples at room temperature were obtained using the LCR meter at 1 kHz. The coercive field (E_c) and remnant polarization (P_r) were determined from P-E hysteresis loops obtained by a RT66A ferroelectric meter.

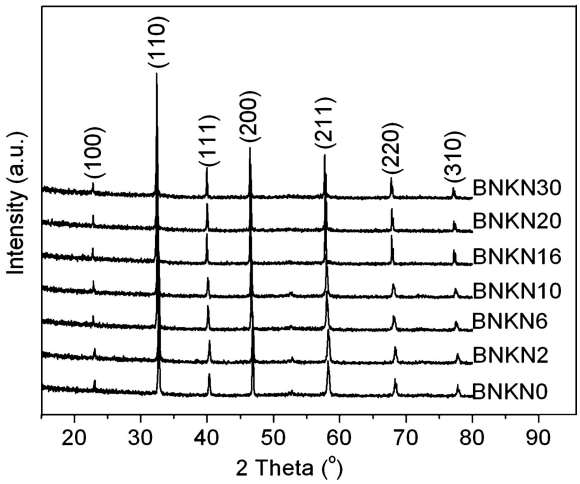

Figure 1 X-ray diffraction patterns for all unpoled BNKN system ceramics at 2θ between 10–80°.

3. Results and discussion

3.1. Crystal structure

The XRD patterns of unpoled BNKN100x (x = 0, 0.02, 0.06, 0.10, 0.16, 0.20 and 0.30) ceramics show a single phase of perovskite structure with a rhombohedral or tetragonal symmetry depending on the content of BKT (Fig. 1). At room temperature, BNT has rhombohedral symmetry, whereas BKT has tetragonal symmetry.

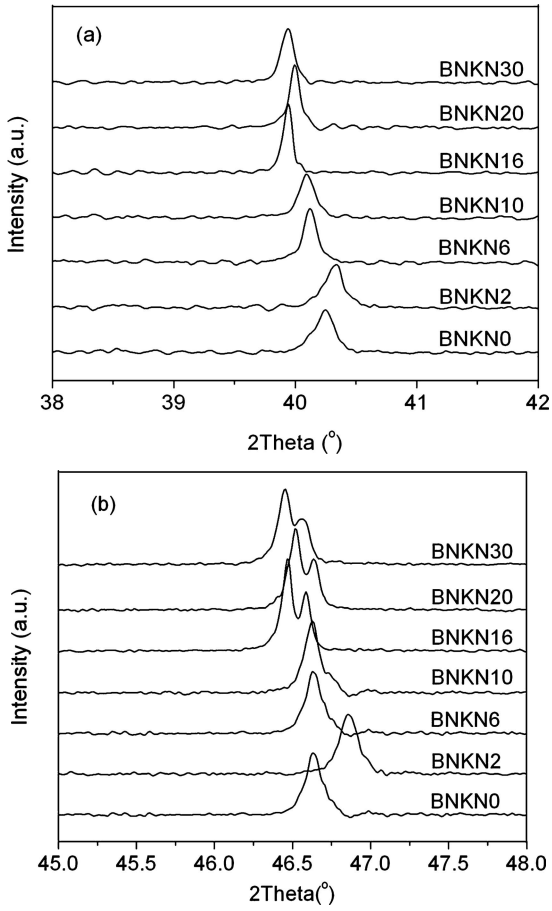

Figure 2 X-ray diffraction patterns for all unpoled BNKN system ceramics at 2θ between (a) 38–42° (b) 45–48°.

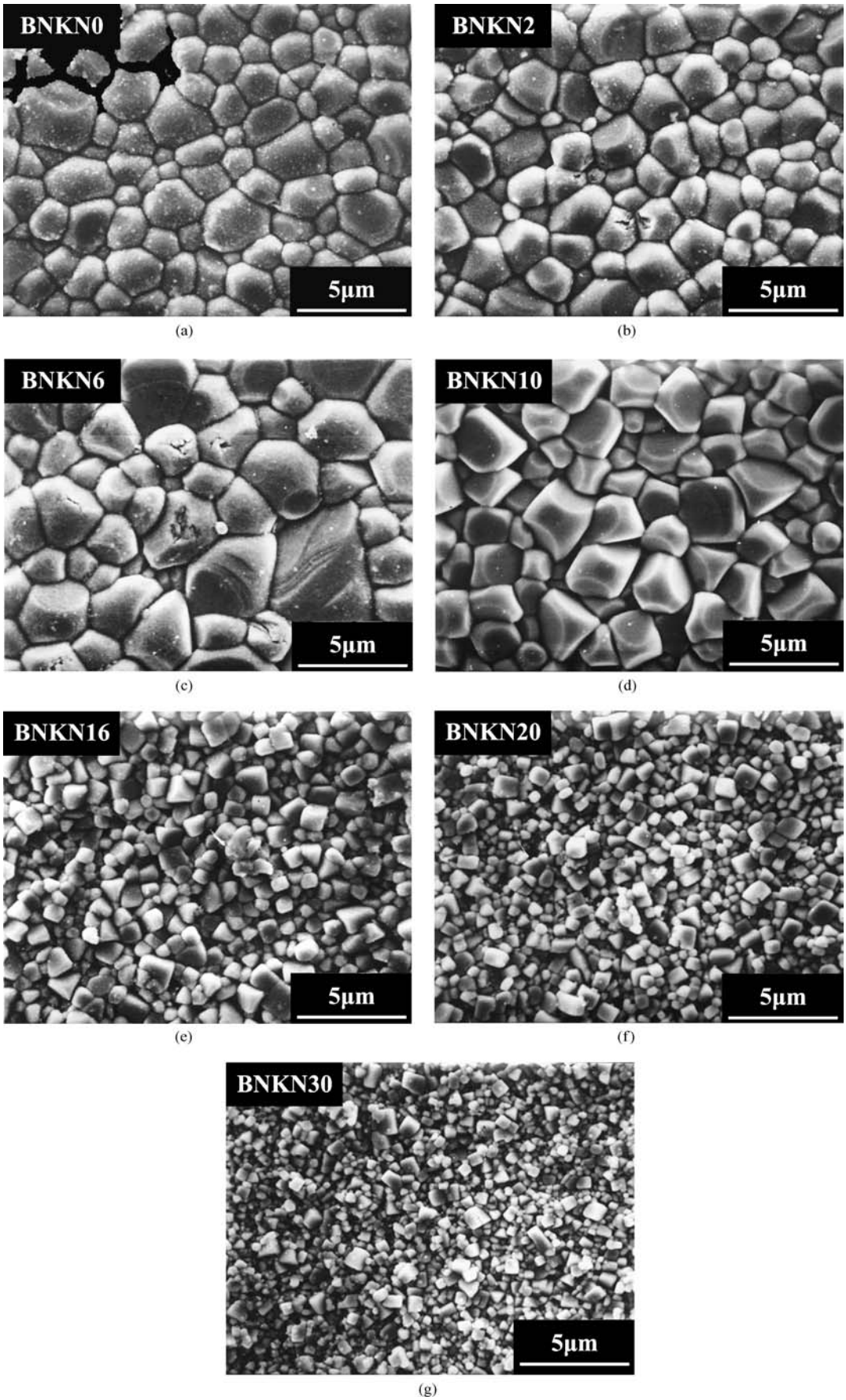

Figure 3 Microstructures of BNKN system ceramics influenced by the amount of BKT.

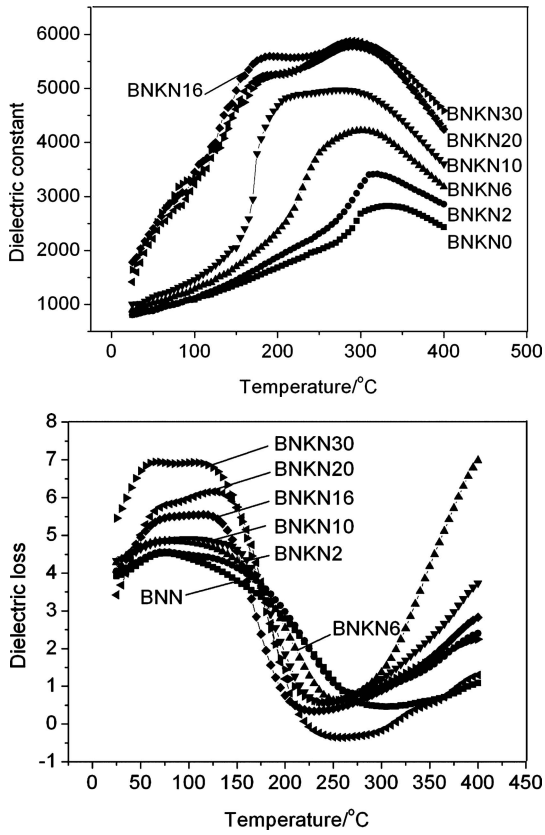

Figure 4 Temperature dependences of permittivity and dissipation factor for all unpoled BNKN system ceramics.

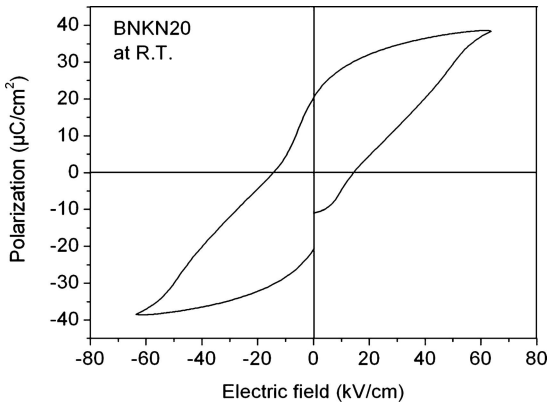

Figure 5 P-E hysteresis loop of BNKN20 ceramic at room temperature.

Therefore, a MPB can be expected to exist in BNKN solid solution. The difference between the two symmetry structures can be seen clearly in the XRD patterns, which were scaned in 2θ ranges of 38–42° and 45–48°, corresponding to the diffraction peaks of (111) and (200) planes, respectively (Fig. 2). It is evident that the samples of BNKN0, BNKN2, BNKN6 and BNKN10 had the same structure of rhombohedral distortion because no splitting of (200) peak (related to tetragonal distortion) was observed. However, the line splitting of (111) peak, corresponding to the rhombohedral distortion, was not observed in these samples, as reported in BNT-$PbTiO_3$ system [16]. It was suggested that the rhombohedral distortion could be detected by XRD only after the ferroelectric microdomain, resulting from the disorder distribution of A-site cations, transformed to macrodomain under electric field forcing. The XRD patterns of BNKN16, BNKN20 and BNKN30 indicated these samples transformed to tetragonal phase, as demonstrated by the splitting of peak (200). Clearly, the phase boundary between rhombohedral and tetragonal phase of BNKN system existed near the point of $x = 0.16$. This result was in good agreement with the following dielectric and piezoelectric datas of the BNKN solid solution.

3.2. Microstructure

SEM micrographs of the surfaces BNKN ceramics are revealed in Fig. 3. It is evident that the content of BKT had great influence on the grain morphology and average grain size. It seemed that BKT addition at amount less than 6 mol% enhanced the grain growth. However, the average grain size decreased with the increase in BKT amount at the addition more than 6 mol%. When the addition of BKT was more than 16 mol%, the samples exhibited much fine grain with inhomogeneous grain size. At the same time, the addition of BKT promoted the growth of square grains, as a result of the large anisotropy of BKT grains. Uniform and fine grain microstructure in BNKN16

TABLE I The electrical and piezoelectric properties of BNKN100x system ceramics

$Bi_{0.5}K_{0.5}TiO_3$ content (x)	0	0.02	0.06	0.10	0.16	0.20	0.30
$\varepsilon_{33}^T/\varepsilon_0$ (1 kHz)	565	512	532	636	1005	1806	1560
$tg\delta$ (1 kHz)	0.031	0.026	0.022	0.024	0.037	0.05	0.048
d_{33} (PC/N)	90	90	97	108	146	30	118
k_p (%)	12.4	18.5	22.6	25.8	30.3	–	18.4
k_t (%)	43.8	48.5	48.4	43.9	53.2	–	50.9
k_t/k_p	3.53	2.62	2.14	1.70	1.69	–	2.77
Q_m	294	232	284	200	104	–	43
T_d (°C)	–	–	–	230	190	180	180
T_m (°C)	337	320	300	278	289	287	283
P_r (μC/cm^2)	42.3	46.9	33.7	35.4	33.2	20.3	22.9
E_c (kV/cm)	54.6	47.1	45.2	41.6	33.2	38.4	17.1

indicated that excellent piezoelectric properties might be obtained.

3.3. Dielectric properties

Fig. 4 shows the temperature dependences of permittivity and dissipation factor of unpoled BNKN100x samples at 1 kHz. The permittivity increased with BKT content in the measuring temperature range and it reached maximum value at the MPB ($x = 0.16$). It also could be seen that all samples exhibited similar dissipation behavior. The dissipation factor of these compositions increased with temperature due to the domain wall motion in the ferroelectric region. After antiferroelectric phase started taking place, the dissipation factor continued diminishing. Above T_m, electrical conductivity began to dominate, resulting in an sharp increase of the dissipation factor. The peak values of dissipation factor increased with BKT content. At low BKT concentration ($x = 0, 0.02, 0.06$), only one broad peak was observed in each sample, corresponding to the diffusive phase transition from antiferroelectric to paraelectric phase. As BKT

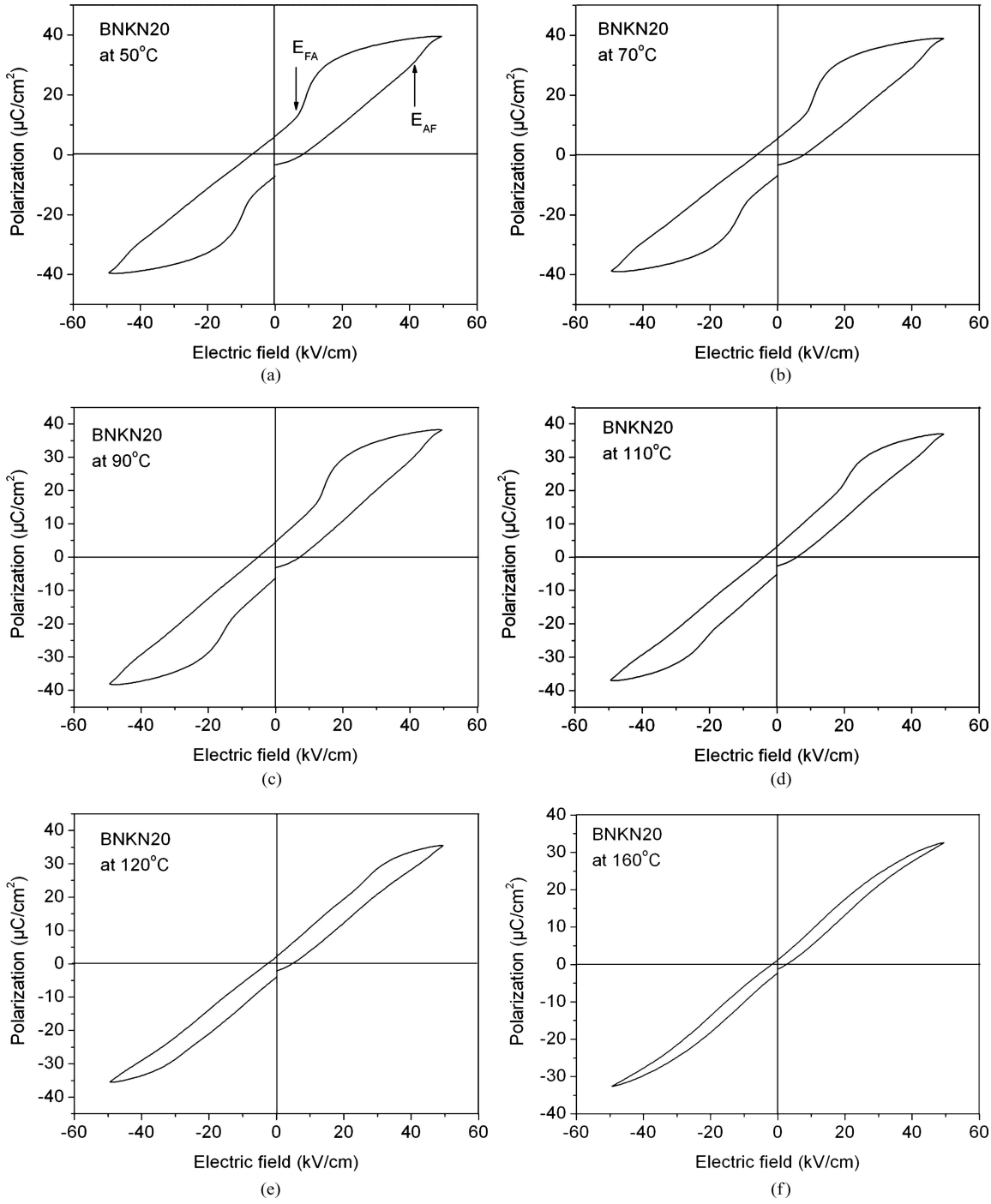

Figure 6 P-E hysteresis loops of BNKN20 ceramic at higher temperatures (50, 70, 90, 110, 120 and 160°C).

concentration increased ($x = 0.10, 0.16, 0.20, 0.30$), there appeared two kinds of dielectric abnormality on the permittivity vs. temperature curves. The distinct hump at T_d was usually regarded as the confirmation of the phase transition from ferroelectric to antiferroelectric phase, as reported in BNT-NN-BT [6], BNT-PT [17]. It was inferred that the BKT addition was in favor of the formation of antiferroelectric phase because T_d shifted to lower temperature when BKT content increased, as listed in Table I. The temperature dependences of permittivity of all samples showed maximum value at T_m, corresponding to the transition from antiferroelectric to paraelectric phase. The temperature dependences of permittivity at different frequencies (100 Hz, 1 kHz, and 10 kHz) were also measured, not shown in this paper. The results showed that the phase transition from ferroelectric to antiferroelectric phase appeared as relaxor characteristic. T_d and the magnitude of ε_r were strongly frequency dependent at all measuring frequencies, i.e. the higher the frequency, the higher the transition temperature, the lower the permittivity. Generally, the relaxor ferroelectric property of BNT is attributed to the long-range disorder of A-site cations, such as Bi^{3+} and Na^{+}. With the addition of BKT, K^{+} preferably entered into A-site and substituted for the isovalent ion Na^{+}. So the disordered distribution of A-site cations was enhanced. Therefore, a more distinct relaxor behavior was observed as the BKT concentration increased.

3.4. Piezoelectric properties

The piezoelectric properties of BNKN system ceramics are listed in Table I. With the increase of BKT content, the piezoelectric properties were enhanced greatly and BNKN16 showed the best piezoelectric properties: $d_{33} =$ 146pC/N, $k_P = 30.3\%$ and $k_t = 53.2\%$. As the composition of BNKN16 is near the MPB, two structures of rhombohedral and tetragonal coexist in this ceramic so that domain is easier to orientate along the electric field direction. With further increasing BKT content, the piezoelectric properties decreased. The anisotropy of electromechanical coupling factors (k_t/k_p) decreased with increasing BKT content and it reached the minimum value when $x = 0.16$. It was also observed that the quality factor (Q_m) values decreased as BKT content increased.

It was worthy to be noted that the BNKN20 ceramic had abnormal piezoelectric properties with $d_{33} = 30$ pC/N and electromechanical coefficients (k_p and k_t) were too small to be measured. The P-E hysteresis loop at room temperature of BNKN20 is shown in Fig. 5 and provides a clue to explain this phenomenon. The P-E hysteresis loop shrinked at the middle, which was different from that of typical ferroelectrics. This was also observed in BNT-PT [16] and 0.97BNBT6-0.03La [18]. It was suggested that some antiferroelectric regions existed in these ceramics so that the P-E hysteresis loop exhibited the characteristic of antiferroelectric to some extent. The existence of antiferroelectric resulted in the decrease of spontaneous polarization as the spontaneous polarization of antiferroelectric is zero on the macroscale. The P-E hysteresis loops of BNKN20 at higher temperatures were measured, as shown in Fig. 6. It was revealed that the transition from antiferroelectric to ferroelectric could take place under the inductive effect of electric field. The antiferroelectric phase was induced to metastable ferroelectric phase at the positive switching electric field E_{AF}, and this ferroelectric phase transformed to antiferroelectric phase again at the negative switching electric field E_{FA} when the electric field decreased. Compared Figs 5 and 6, it was shown that E_{AF} increased a little as the temperature increased, while E_{FA} increased rapidly with increasing temperature. This was attributed to the fact that the stability of this metastable ferroelectric phase decreased with increasing temperature, resulted from the enhancement of thermal fluctuation of dipole in ferroelectric domain. Accordingly, the ferroelectric phase tended to transform to antiferroelectric phase as temperature increased.

4. Conclusion

All compositions investigated in this work could form single perovskite phase. It was proved by X-ray diffraction that the morphotropic phase boundary between rhombohedral and tetragonal phase of BNKN system existed at the point of $x = 0.16$. The amount of BKT was found to affect the grain size and morphology. From room temperature to 400°Cl compositions experienced two phase transitions: from ferroelectric to antiferroelectric at the first transition temperature T_d and from antiferroelectric to paraelectric at T_m. At low concentration of BKT ($x = 0$, 0.02 and 0.06), only one broad peak was found, corresponding to the transition from antiferroelectric to paraelectric phase. As BKT concentration increased, there appeared a distinct hump at T_d, corresponding to the phase transition from ferroelectric to antiferroelectric phase. And T_d shifted to lower temperature when BKT content increased. Transition from ferroelectric to antiferroelectric exhibited relaxor characteristic. The piezoelectric properties of ceramics were enhanced greatly with the increase of BKT content and BNKN16 showed the best piezoelectric properties: $d_{33} = 146$ pC/N, $k_P = 30.3\%$ and $k_t = 53.2\%$. BNKN20 had abnormal piezoelectric properties due to the co-existence of ferroelectric and antiferroelectric phase in this ceramic at room temperature. The antiferroelectric phase could be induced to metastable ferroelectric phase by electric field, and the electrically induced ferroelectric phase would transform to antiferroelectric phase when the electric field decreased.

References

1. G. A. SMOLENSIKII, V. A. ISUPOV and A. I. AGRANOVSKAYA, *Sov. Phys.-Solid State (Engl.Transl.).* **2** (1961) 2651.
2. T. TAKENAKA, K. MARUYAMA and K. SAKATA, *Jpn. J. Appl. Phys.* 9B **30** (1991) 2236.

3. K. SAKATA, T. KAKENAKA and Y. NAITOU, *Ferroelectrics*. **131** (1992) 219.
4. J. SUCHANICZ, M. G. GAVSHIN and A. Y. KUDZIN, *J. Mat. Sci*. **36** (2001) 1981.
5. M. L. ZHAO, W. L. ZHONG and C. L. WANG, *Acta Phys. Sinica*. **51** (2002) 1856.
6. Y. G. WU, H. L. ZHANG and Y. J. ZHANG, *Mat. Sci*. **38** (2003) 987.
7. T. TAKENAKA, T. OKUDA and K. TAKEGAHARA, *Ferroelectrics*. **196** (1997) 175.
8. H. NAKADA, N. KOIZUMI and T. YAKENAKA, in Proceeding of the Electronics Division Meeting of the Ceramics Society of Japan, 18th, 1999, 37–40.
9. H. NAGATA and T. TAKENAKA, *Jpn. J. Appl. Phys*. **9B, 36** (1997) 6055.
10. *Idem. ibid*. **9B, 37** (1998) 5311–5314.
11. A. HERABUT and A. SAFARI, *J. Am. Ceram. Soc*. **80** (1997) 2954.
12. X. X. WANG, H. L. CHAN and C. CHOY, *Solid State Communication*. **125** (2003) 395.
13. A. SASAKI, T. CHIBA and Y. MAMIYA, *Jpn. J. Appl. Phys*. **9B, 38** (1999) 5564.
14. H. NAGATA, M. YOSHIDA and Y. MAKIUCHI, *ibid*. **42** (2003) 7401.
15. M. ONOE and H. JUMONJI, *J. Acoust. Soc. Am*. **41** (1967) 74.
16. S. KUHARUNGRONG and W. SCHULZE, *J. Am. Ceram. Soc*. **79** (1996) 1273.
17. S. KUHARUANGRONG, *J. Mat. Sci*. **36** (2001) 1727.
18. H. D. LI, C. D. FENG and P. H. XIANG, *Jpn. J. Appl. Phys*. **32** (2003) 7387.

Received 23 September 2004
and accepted 22 July 2005